EFDA–JET–CP(06)04–26

D.J. Wilson, D. Ciric, S.J. Cox, T.T.C. Jones, M. Kovari, A. Li Puma, D. Martin,
J. Milne, M. Shannon, E. Surrey and JET-EFDA Contributors

Physics Basis and Mechanical Design of the Actively Cooled Duct Scraper Protection for the JET Neutral Beam Enhancement

Physics Basis and Mechanical Design of the Actively Cooled Duct Scraper Protection for the JET Neutral Beam Enhancement

D.J. Wilson[1], D. Ciric[1], S.J. Cox[1], T.T.C. Jones[1], M. Kovari[1], A. Li Puma[2], D. Martin[1], J. Milne[1], M. Shannon[1], E. Surrey[1] and JET-EFDA Contributors*

[1]UKAEA Fusion/Euratom Association, Culham Science Centre, Abingdon, Oxon, OX14 3DB, U.K.
[2]Association EURATOM-CEA, CEA-Cadarache, 13108 St. Paul-Lez-Durance, France
**See annex of J. Pamela et al, "Overview of JET Results",*
(Proc. 20th IAEA Fusion Energy Conference, Vilamoura, Portugal (2004).

Preprint of Paper to be submitted for publication in Proceedings of the
SOFT Conference,
(Warsaw, Poland 11th – 15th September 2006)

ABSTRACT
The objectives of the JET Neutral Beam Enhancement (NBE) include raising the delivered power from the present 25MW to >34MW and increasing the pulse length from 10s to 20s. The additional power will be obtained partly by increasing the fractional energy components of the beam, resulting from acceleration of molecular ions, hence increasing the total particle flux. These changes place extreme demands on the design of the upgraded protection to the torus entry duct. The present inertial duct protection already reaches its thermomechanical limit in 10s pulses, and active cooling of the upgraded duct protection is therefore essential. Extensive analysis of the pressure and temperature evolution in the present un-cooled duct established the relationship between gas re-emission and surface temperature for copper in this operating environment. This information was used in an integrated physics and engineering approach to the design of the actively cooled duct protection, taking into account the power loads from direct beam interception and re-ionisation. Surface temperature determines power density through the gas re-emission and consequential beam reionisation. These considerations define the normal operating point for the chosen enhanced hypervapotron element technology. This approach demonstrated that supplementary *in-situ* duct cryopumping would not be needed, provided that the required heat-transfer performance could be met without any encroachment of the elements beyond the space envelope of the existing inertial duct protection plates. This requirement posed severe constraints on the mechanical design of the hypervapotron element array and its manifolding; the adopted engineering design solutions are presented.

1. INTRODUCTION
The essential role of the JET beamline duct protection is to accept power from directly-intercepted neutral particles in the fringe of the beams (“scraping” action) and from re-ionised beam particles produced by collisions of the beam neutrals with background gas. Re-ionisation occurs along the entire neutral beam path length downstream of the deflection magnet. The ions thus formed are focused onto the vertical side protection plate (acting as duct “liner”) in the gradient of the steeply increasing vertical magnetic fringe field as the beam passes through the torus entry port. Due to the intrinsic focusing action, which is a universal feature of co-injected beams, the power densities on the vertical side of the duct protection often become high (>5MWm-2), even at the moderate duct vacuum pressures characteristic of a clean and well-conditioned duct. The presently-operating duct scraper/liner assembly (installed 1993 and extended 1995) relies on thermal inertia, with heat removal by water cooling tubes brazed on the back-side and/or radiation. The Neutral Beam Enhancement (NBE) will result in a 50% increase in transmitted beam power (at a maximum beam energy of 125kV), combined with a 35% increase in beam particle flux compared with the highest-flux (80kV) beams used to-date. Re-ionisation power scales with both power and duct pressure which in turn depends on particle flux, and the total deposited energy scales with pulses-length which is to be doubled from 10s to 20s. One of the two JET beamlines, operating at predominantly 80kV, already produces surface temperatures of >500^{o}C on the inertial duct liner, reaching its thermomechanical

operating limit. Scaling this result to the expected NBE performance values implies >900^{o}C would be reached in 20s pulses for the existing duct protection; this implies full active cooling is needed.

2. PHYSICS DESIGN

The key physical consideration defining the required heat-transfer performance of the duct protection is the relationship between surface temperature and rate of gas emission from the surface under bombardment by re-ionised beam particles. Since there is a link between gas source rate and re-ionised power fraction through the duct pressure, an instability threshold exists in the duct gas-balance [1]. This may be expressed as a critical gas re-emission coefficient Gcrit, defined as the ratio of re-emitted molecules to incident ions. Gcrit decreases with beam particle flux and increases with effective duct pumping speed. For NBE Gcrit will be < 3 without additional *in-situ* pumping, a condition more demanding than for any neutral beam duct ever operated. Analysis of the duct pressure evolution in the existing JET NB ducts from the pre-beam phase (when the only gas source is from the gas-feed to the ion-sources, neutralisers and torus) followed by the beam-on phase allows the value of the gas re-emission coefficients G for direct interception and re-ionisation to be inferred [1]. Since the predominant beam energy is presently different on the two beamlines (80kV and 130kV respectively), this permitted a comparison of the values of G for low particle flux (130kV) and high flux (80kV) at a given surface temperature. The values of G for the high flux (80kV) case were systematically lower than for the low flux case. This implies that a simple re-emission coefficient does not describe the physical situation satisfactorily. However, the data for the the low- and high-flux cases is brought together by assuming a constant value G=0.5 for beam particle re-emission (i.e. ideal balance) plus a simple thermal outgasing rate (Q mbar.l/s) with linear surface temperature (T) dependence (Fig.1). This data permitted the derivation of self-consistent values of duct pressure, re-ionisation power density and surface temperature of the actively cooled element. The calculation required a trajectory-tracing code for re-ionised particles in the fringe magnetic fields for a range of operating scenarios, and for direct interception of neutrals. The self-consistent calculation took into account the total gas source from the gas feeds, from direct interception/re-ionisation particle re-emission, and from thermal outgasing Q(T) (Fig.1), together with the curve characterising power density versus T for a linear assembly made from MAST-type hypervapotron elements [2] (see section 3). The typical normal operating condition is predicted to be at moderate values of surface temperature (<200^{o}C) and power density (≈$6MWm^{-2}$), thus providing significant margin for transients in off-normal events.

3. ENGINEERING DESIGN

All the present duct protection panels (see figure 2) including their water manifolding and thermocouple attachments are internally mounted inside a stainless steel conical support structure that is cantilevered from the Mid Port Adaptor (MPA) assembly, which is in turn attached to the Main Horizontal Port (MHP), where the primary vacuum joint to the Torus Vacuum Vessel is made (see figure 3). The MPA allows attachment of the main Neutral Beam Boxes (via large bore rotary isolation valves) and the inclusion of diagnostics, electrical and cooling water feedthroughs. The MPA and part of the MHP are heated using external cables up to 320^{o}C during vessel conditioning (400^{o}C maximum allowable) and are covered with insulating material to help with this. The complete duct protection assembly, apart from some additional uncooled in-vessel tiles that are mounted at the top and bottom of the port throat, can be effectively removed from the MHP using a special balanced lifting beam. It is necessary to replace only the vertical left and right hand inertial side panels with actively cooled assemblies. These new assemblies will be incorporated into the existing structure and are therefore subject to very restrictive geometrical constraints. The final scheme design selected for the new side panels, is one that uses six horizontally orientated hypervapotron elements, made from CuCrZr (see figure 4). Each element is connected to a single vertical, bi-directional flow manifold, that combines both the cooling water inlet and return feeds. The top and bottom elements include solid extensions that overlap with the existing solid OFHC copper panels at the corner regions of the stainless steel conical support. Water can be circulated in either direction, which means that only one panel design is necessary to fit in both locations.

Attachment of the new side panels to the existing conical support structure uses three vertical brackets per panel, with three M12 screws fixing each individual hypervapotron element to them. The large thermal gradients between the heated port structures (~200^{o}C in normal operation) and the water-cooled side panels (~18-23^{o}C with no beam loading) are catered for using a captured aluminium bronze bush and slot arrangement. Small movements of the elements into the port are possible, but these are limited to the compression of several captured disc springs (~0.86mm/disc at 75% compression) at the fixing screws. It is necessary to maintain the panel profile (see figure 5) and to preserve a simple interlocking feature on the sides of each element. This provides a labyrinth that protects the rear structures from beam shine-through, with the nominal gap set at 1.5mm between elements. The scraper panels must be secured to the main structure at their attachment points in order to withstand the considerable forces that are experienced during disruptions. These could be as high as 7g, 3.5g and 2g in the radial, toroidal and vertical directions respectively and are compounded with electromagnetic torques from induced eddy currents from the magnetic field changes in the region. The main advantages of the final scheme design selected over the many that were investigated are summarised by the following points:-

- The individual water flow circuits are more evenly balanced for heat removal with equal, relatively low pressure drops
- Port encroachment is minimised, requiring the element total thickness to be reduced to ~18-20mm in places. Exposed edges are avoided.
- It allows construction of ‘one off’ duct liner panels that fit both the left and right hand positions.
- The basic MAST type hypervapotron elements adopted [2] (although slightly modified), have been extensively tested at much higher steady state power loadings (18MW/m^{2}),

than required for this application.

- A low front face panel temperature is the prime design requirement (<200^{o}C) which is achieved with a modest (with respect to hypervapotron elements) flow velocity of 6.25m/s. Run-away in the re-ionised particle loads are avoided if this temperature is maintained.
- The fabrication sequence envisaged, uses known technologies and materials that have been already used for JET NBI components and selected for this reason.
- The impact on existing structures should be minimal, with significant re-use of original components.
- There are no weak components (eg. bellows, brazed joints) in this design, that would be more susceptible to failure from direct power loads, than others.

4. ENGINEERING ANALYSIS

Pressure drop calculations using analytical formulas predict total pressure drops of 0.41MPa for each of the internal scraper side panel assemblies (0.35MPa occurs in the 2.4m long hypervapotron circuit), at the design point total water flow of 22.5m^3/hr per panel (~1 litre/sec per element) [3]. A pressure of 11 bar absolute (1.1MPa) has been selected for the ASME VIII Div2 design criteria. These estimates are obtained by linearly combining singular losses at each discontinuity (elbow, section reduction and enlargements, splitting, regrouping…). The validity of this method is being crosschecked with a preliminary experimental mock-up and later on at the contract manufacturing stage with the testing of a prototype assembly.

Thermal performance (see table 1) is based on a maximum heat flux (HF_{max}) applied on the beam side surface (for a period of 20s), from a combination of the following components used to generate power density profiles along the length of an individual scraper element:-

a) Direct Beam Interception (total thermal load on the entire right hand side panel of ~202kW, equating to a linear distribution with a maximum at 0. 85MW/m^2).
b) Beam re-ionisation from beam-gas collisions (three different scenarios assessed)
   - A homogeneously distributed HF from gas re-ionisation, of 3.62MW/m^2 [Case1], a 6MW/m^2 hot spot [Case2] and a 12MW/m^2 hot spot [Case3]. Re-ionisation power has been scaled from thermocouple measurements for cases 2 & 3.
c) Plasma Facing Radiation of 0.3MW/m^2 as per [4].

The steady state maximum temperature is reached on the cooled section of the element in ~2.5s, but the plasma facing un-cooled region of the element does not reach equilibrium during the 20s pulse. In the unlikely event of 100% beam blockage of the port, the expected heat flux of 100 MW/m^2 implies that the front face would reach 1100^{o}C after 100ms. A temperature of 442^{o}C is reached after 15ms (450^{o}C is used as the creep ageing limit for CuCrZr) and implies appropriate beam control response times from duct overpressure trips must be better than this [3]. This is within the capability of the JET Fast Beam Interlock System fail-safe protection network [5], although it is likely that the speed of response of the front end measurement sensor (presently a Penning gauge) may have to be improved, or supplemented with e.g. an optical measurement.

Structural analysis of the vertical water manifold and horizontal elements has been made using the ANSYS Finite Element code, with the computed stresses checked according to the ITER structural design criteria (SDC-IC). With a 75/35 MPa inlet/outlet pressure split in the manifold, the maximum membrane stress is 18 MPa (cf. Sm limit = ~110MPa), while the maximum membrane plus bending stress is 72 MPa (cf. 1.5Sm = ~170MPa. These linearised primary stresses are everywhere below the limits assumed for plastic collapse or instability in this material.

A model of an entire hypervapotron element, including the additional *secondary stresses* due to temperature gradients and limited displacements and *primary stresses* due to internal pressure, acceleration and electromagnetic torque was analysed. In the three assessed scenarios the thermal stresses are localised where the maximum temperature occurs in the front face. In the worst case (Case 3) the thermal stresses reached 298 MPa with total stresses up to 310 MPa, which satisfies the 3Sm rule, so guaranteeing against progressive deformation of the component). Element displacement towards the beam reaches a maximum (Case 1) at ~3mm (3.16mm during a disruption) which is an acceptable encroachment. Due to the elements' geometry (1.2m length with a 4mm front face thickness), further refinements of the already very large model to find the peak stresses is ongoing.

Fatigue life estimation has not as yet been performed, however the obtained stresses and temperatures are far lower than those estimated for the MAST hypervapotron elements.

5. FUTURE PROGRAMME

Thermal and structural analysis is continuing with a focus on evaluating peak stresses, the effect of the axis of symmetry used compared with the actual split flow design and cross-checking of the stresses obtained by applying displacement fields as boundary conditions.

The fabrication sequence is a critical element of the design and requires that the manufacture contract include an initial phase of prototype construction and testing, together with pre-qualification of the anticipated joining methods and procedures, before final manufacture of the production assemblies is started. Contracts for the detailed design and manufacture of the MkIII scraper panels are planned to be in place by Jan 2007, with completion of the first prototype stage by Oct 2007 and delivery of the final panels for installation on the JET Torus by July 2008.

SUMMARY AND CONCLUSIONS

The fundamental constraints imposed by the MHP vacuum vessel aperture, especially at the throat of the port are particularly severe and are a limitation for the JET Neutral Beam heating system. The space available for duct protection is very tight, which leaves little scope for innovative designs. Further encroachment into the duct is self-defeating and would result in less neutral beam power being injected into the plasma due to the increased direct scraping of the beams. Performance of the present inertial duct scraper protection is the limiting factor in neutral beam delivery, with PINI trips on duct overpressure, associated with high surface temperatures, a common occurrence for the longer injection times. The proposed hypervapotron elements have a much higher power handling capacity (a factor of 3), than that predicted for the peak power densities due to focusing of particles in the poloidal fringe fields. This robustness in power handling is necessary when considering possible power loads that might occur during certain fault condition scenarios. This design provides an acceptably low front face temperature (<200°C) according to the self-consistent integrated physics/engineering predictive model adopted. This limits the amount of outgasing, which could otherwise lead to a runaway in the re-ionised component of the incident power loading, if temperatures were allowed to increase. CuCrZr is the only beam facing material. It has a proven track record on JET and MAST and is proposed for useon ITER. Electron beam welding in the solution heat-treated state, is the proposed method of fabrication and is well defined.

ACKNOWLEDGEMENT

This work has been conducted under the European Fusion Development Agreement and is partly funded by the United Kingdom Engineering and Physical Science Research Council and by the European Commission under the Contract of Association between Euratom and UKAEA. The views and opinions expressed herein do not necessarily reflect those of the European Commission.

REFERENCES:

[1]. "Beamline duct gas release/conditioning and the upgraded duct wall protection system of the JET neutral injectors". A J Bickley *et al.*, 13th IEEE/NPSS Symposium on Fusion Engineering, SOFE 1989, Knoxville, Tennessee, p 1438

[2]. "Hypervapotron design for the Long Pulse upgrades on MAST NBI", J. Milnes *et al.*, 20th IEEE/NPSS Symposium on Fusion Engineering, SOFE 2003, San Diego, pp. 478-481

[3]. "Analysis of Actively Cooled Duct", Internal Culham Division technical report CD/EP2-NBE-Mech/T/003, Issue 1-July 2006, A. Li Puma, Engineering and Cryogenics Group

[4]. "Operation and Fault Condition Design Criteria for JET Components", Internal Culham Division Procedure CD/S/J031 Issue 2, June 2006

[5]. "The Fast Beam Interlock System for JET Neutral Injection", D Cooper *et al.*, 12th IEEE/NPSS Symposium on Fusion Engineering, SOFE 1987, Monterey, California, pp 1096 - 1100.

Power Density Profiles	HF_{max} [MW/m^2]	Total Integrated Power [single element] [kW]	Water T_{out}, [°C]	CuCrZr T_{max}, [°C]
Case 1	4.47	212.3 (~40% of total power on RHS scraper panel)	80	203
Case 2	6.08	57.5	44	153
Case 3	12.45	113.8	56	299

Table 1 Thermal analyses, loading conditions and results

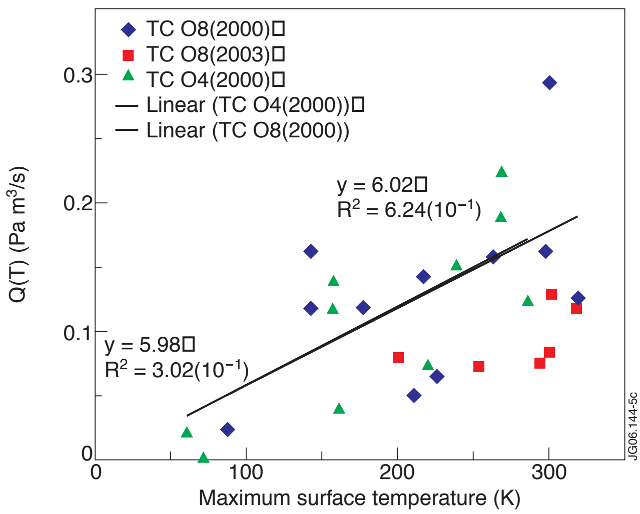

Figure 1: Thermal outgasing rate Q vs. thermocouple (TC) temperature (T) for inertial copper duct liner (O8: 130kV low flux; O4: 80kV high flux cases) based on measurements taken in the campaign years indicated. The linear fit parameters and correlation coefficients for separately fitted O8 and O4 data are as shown.

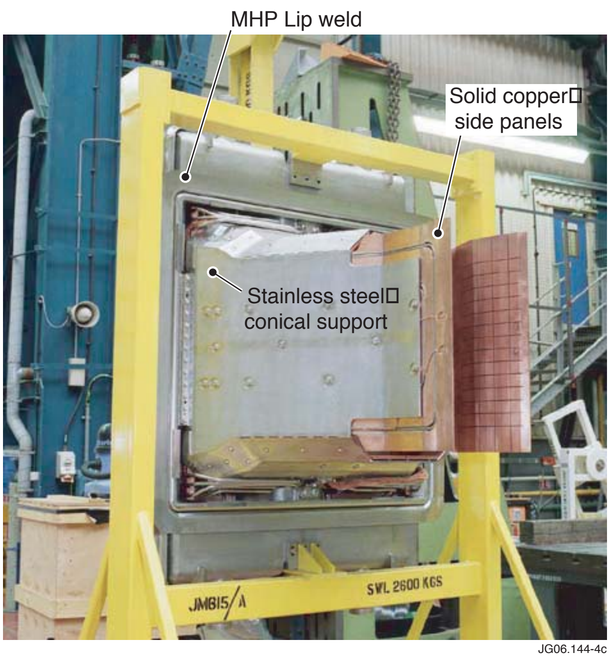

Figure 2: Existing Inertial Duct Protection shown mounted inside of conical support structure attached to MPA.

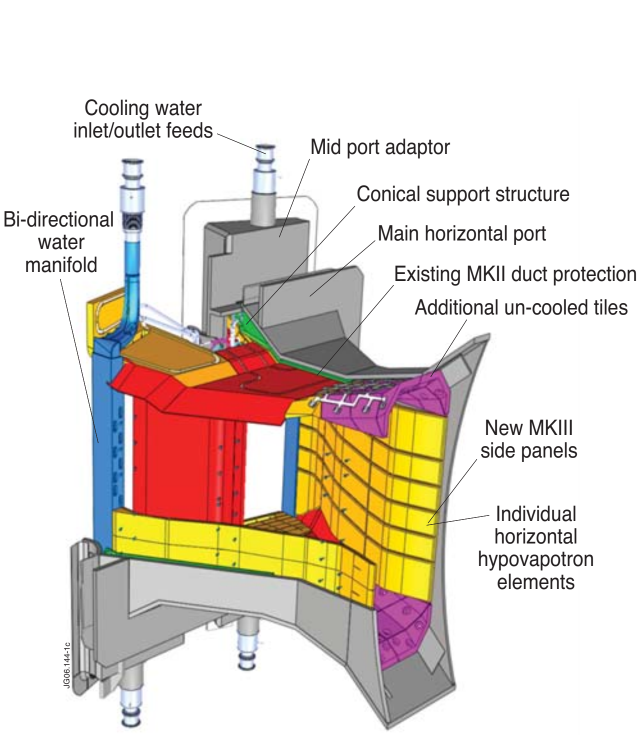

Figure 3: Section through MHP showing internal duct protection orientation

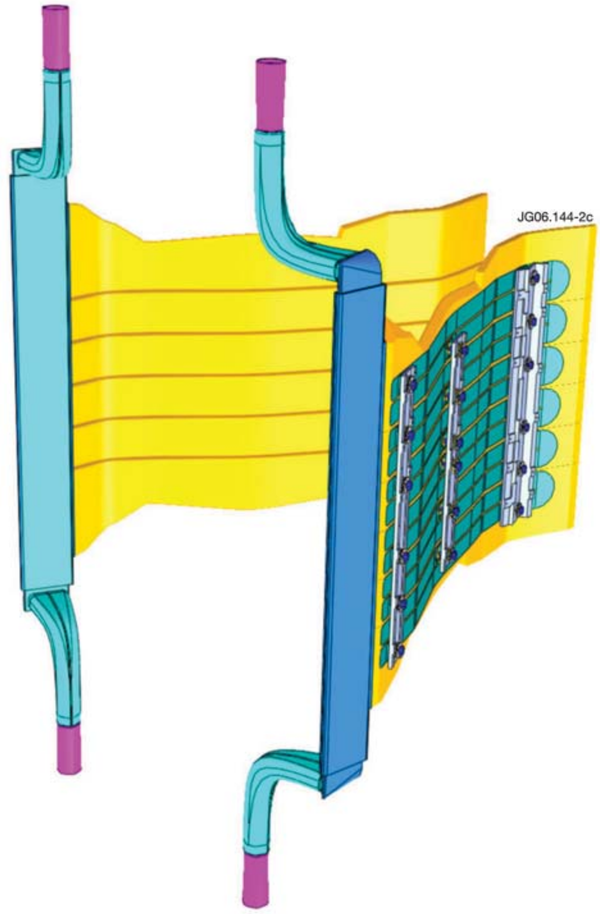

Figure 4: Scheme Design of the new MkIII actively cooled Duct Scraper left and right hand side panels

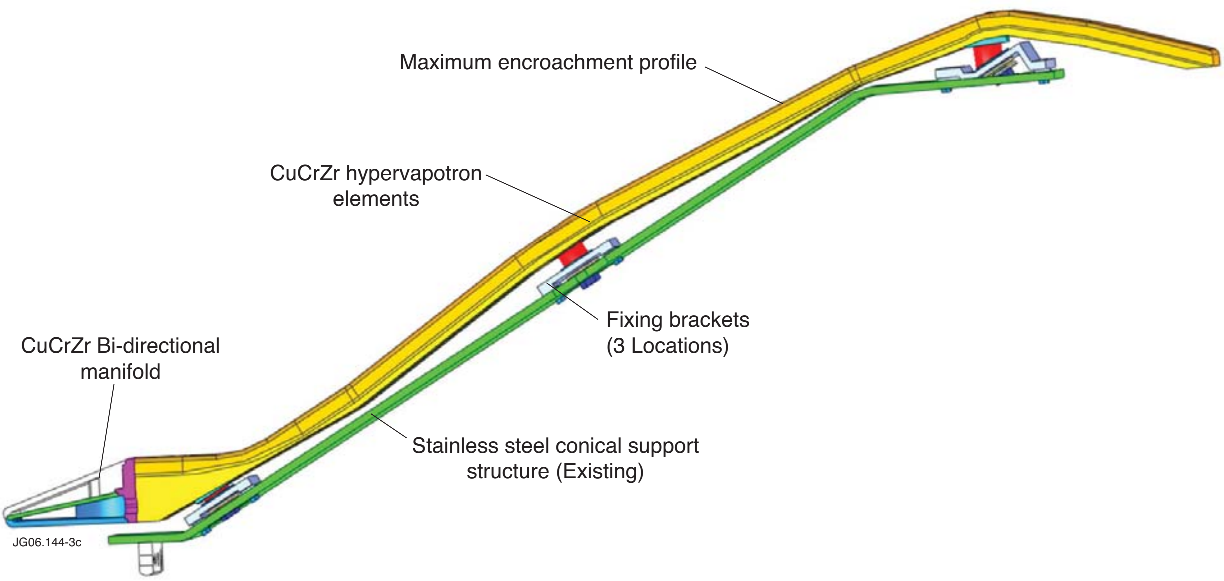

Figure 5: Profile of New MkIII right hand side panel